AFM-Based Fabrication of Nanofluidic Device for Medical Applications

R. Promyoo[*], H. El-Mounayri[*,***], V.K. Karingula[*] and K. Varahramyan[**]

[*]Department of Mechanical Engineering, Indiana University Purdue University Indianapolis, IN, USA
[**]Department of Electrical and Computer Engineering, Integrated Nanosystems Development Institute, Indiana University Purdue University Indianapolis, IN, USA
[***] Corresponding author (helmouna@iupui.edu)

ABSTRACT

Recent developments in science and engineering have advanced the atomic manufacturing of nanoscale structures, allowing for improved high-performance technologies. Among them, AFM-based nanomachining is considered a potential manufacturing tool for operations including machining, patterning, and assembling with in situ metrology and visualization. In this work, atomic force microscopy (AFM) is employed in the fabrication of a nanofluidic device for DNA stretching application. Nanofluidic channels with various depths and widths are fabricated using AFM indentation and scratching techniques. To introduce the fluid inside the nanochannels, microchannels are made on both sides of the nanochannels. Photolithography technique is used to fabricate microfluidic channels on silicon wafers. A 3D Molecular Dynamics (MD) model is applied to guide the design and fabrication of nanodevices using nanoscratching. The correlation between the scratching conditions, including applied force, scratching depth, and distant between any two scratched grooves and the defect mechanism in the substrate/ workpiece is investigated. The MD model allows proper process parameter identification resulting in more accurate nanochannel sizes.

Keywords: Molecular Dynamics, MD, AFM

1 INTRODUCTION

Atomic force microscopy (AFM) has been recently used to fabricate a broader range of structures with higher complexity, greater precision and accuracy. In AFM-based nanomachining, the AFM tips are used as cutting tools for surface modification. Depth and size of indents can be controlled by varying applied forces on AFM tips. AFM-based nanomachining has been applied to several applications such as individualized biomedicine and drug delivery, molecular reading and sorting, ultrahigh density memory, nanoscale circuitry, and fabrication of metal nanowires [1-11]. One of the applications considered in this study is the fabrication of nanofluidic devices in which the nanochannels are fabricated by AFM-based nanoscratching. Nanoscale channel is mainly used in the study of molecular behavior at single molecule level. The most promising application with nanochannels is in the analysis of DNA. Several studies on DNA analysis show that degree of DNA is inversely proportional to the channel dimension due to confinement effects. The interaction of DNA molecules with the nanochannels at persistence length has led to a new way of detecting, analyzing and separating these biomolecules [12].

In this paper, A 3D Molecular Dynamics (MD) model is applied to study the AFM-based nanoscratching process. The correlation between the scratching conditions, including applied force, scratching depth, and distant between any two scratched grooves and the defect mechanism in the substrate/ workpiece is investigated. The simulation allows for the prediction of normal force at the interface between an indenter and a substrate. In addition, AFM-based fabrication of nanofluidic devices is conducted. Nanochannels are fabricated by directly scratching on substrate surface with different applied forces, scratching length, and feed rate.

2 METHODOLOGY

A photolithography process is used to create microchannels on top of the silicon wafer. These microchannels are served the medium as inlet and outlet for the nanochannels. Figure 1 shows the chrome-coated photomask which is used to transfer the image of the microchannels onto silicon substrate. Photomask has a dark chrome side and a transparent side. When the light is exposed, it travels through the transparent medium and strikes the photoresist (AZ-1518). The exposed surface becomes harder and can be removed by using a photoresist developer (MF-26A).

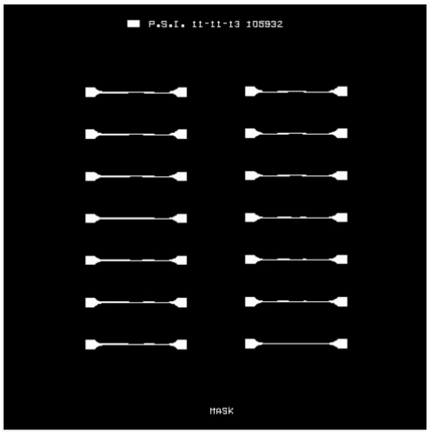

Figure 1: Photomask

The photomask shown in Figure 1 is consist of fourteen devices. Each device has two microchannels and the gap between the two microchannels is approximately 4 micrometers. Reaction ion etching (RIE) is used to remove the uppermost layer of the silicon wafer in the areas that are not covered by photoresist. After the etching process, micro-channels are formed. Then, nanochannels are created between the two microchannels in each device using AFM-based nanoscratching process.

2.1 MD Simulation Model

A 3D Molecular Dynamics (MD) model is applied to guide the design and fabrication of the nanochannels. MD simulations of AFM-based nanomachining in this study are implemented using LAMMPS (Large-scale Atomic/ Molecular Massively Parallel Simulator) [13,14]. The schematic model used in the MD simulation of AFM nanoscratching is shown in Figure 2. The simulation model consists of a single crystal workpiece and a three-sided pyramidal indenter. A diamond indenter tip is selected. The workpiece in the MD simulation is divided into three different zones: boundary, thermostat, and the Newtonian zones. A few layers of boundary and thermostat atoms are placed on the bottom side of the workpiece. Fixed boundary conditions are applied to the boundary atoms. The atoms are fixed in the position to reduce the edge effects and maintain the symmetry of the lattice. Periodic boundary conditions are maintained along the x- and y-direction. The thermostat zone is applied to the MD simulation model to ensure that the heat generated during the indentation process can be conducted out of the indentation region properly. The temperature in the thermostat zone is maintained by scaling the velocities of the thermostat atoms for each computational time step. In the Newtonian zone, atoms move according to Newton’s equation of motion.

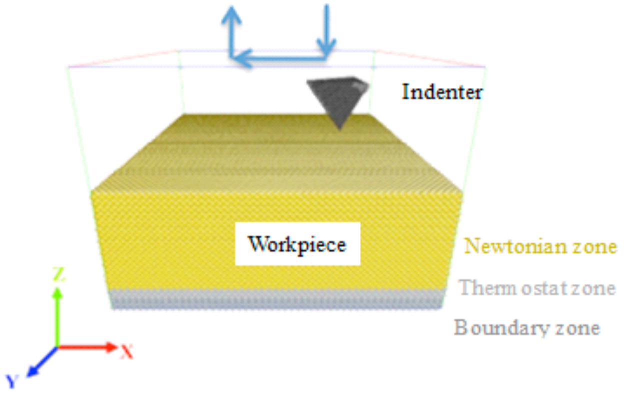

Figure 2: Schematic MD simulation model of AFM nanoscratching

The motion of the atoms in the Newtonian zone is determined by the forces derived from the potential energy function and Newton’s equation of motion. The interaction of each atom can be approximated by a potential energy function in accordance with Newtonian mechanics. The quality of the MD simulation results depends on the accuracy of the potential energy function used. On the other hand, the complexity of the potential energy function directly affects the computational time [15]. The selection of the potential function depends on the type of material used in the model. Tersoff potential [16] is employed for both interactions between silicon atoms in the workpiece material (Si-Si) and between silicon and carbon (Si-C) atoms.

2.2 AFM Experimental Setup

A Veeco Bioscope AFM was used to create nano-channels by directly scratching on the surface of workpiece material. The AFM provides resolution on the nanometer (lateral) and angstrom (vertical) scales. A diamond probe (Bruker DNISP indentation probe) with a spring constant of 250 N/m was used in the experiments. The indenter tip has three-sided pyramid shape. Nanoscratching is performed by forcing the tip into the workpiece until the required cantilever deflection is reached. The tip is then moved horizontally for a specified length and then lifted to its initial position above the workpiece. Nanoscratching can be performed at various forces and rates, using the deflection of the cantilever as a measure of the forces. The nanoscratching experiments were conducted at various applied forces.

3 RESULTS AND DISCUSSION

MD simulation results of AFM nanoscratching are presented in this section. All MD simulation snapshots are visualized by Atomeye [17]. The different colors shown in the following MD simulation figures represent coordination number, which is a measure of how many nearest neighbors exist for a particular atom. The purpose of using this coordination number coloring is to clearly see the defects and dislocations of atoms.

The effect of scratching depth on material deformation was investigated. MD simulations of nanoscratching were conducted with scratch depths varying from 1 to7 nm. Figure 3 show top views of MD simulation snapshots of nanoscratching at various scratching depths. As the scratching depth increases, the deformation is found to penetrate much deeper from the surface and the height of material pile-up also increases. In addition, more dislocation loops on the top surface can be observed. Several types of defects, including vacancies and Shockley partial dislocation loops, can be observed during the simulation. The dislocation loops are highly mobile and participate in various interactions among themselves and with other defects. The dislocation loops on the top surface are emitted in front of the tip and generally move out of the computation domain at a side boundary and come inside from the opposite side of boundary, due to the periodic boundary conditions applied to all four side boundaries.

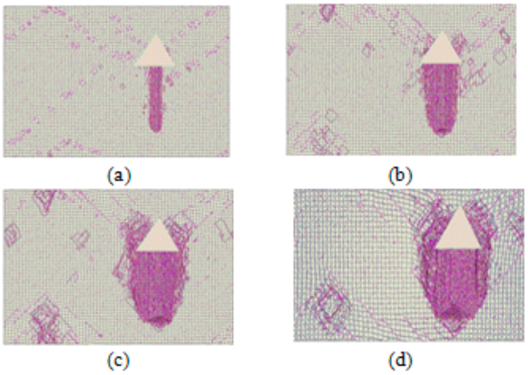

Figure 3: Top view of MD simulation snapshots of nanoscratching with different depths of scratch: (a) 1 nm; (b) 3 nm; (c) 5 nm; (d) 7 nm

MD simulations of nanoscratching were also conducted to find the minimum distant between any two scratched grooves so that the first groove is not affected by the dislocation emitted during scratching of the second groove. Figure 4 depicts MD simulation snapshots of nano-scratching with depth of 5 nm and distances of 1.5, 2.0, 2.5, 3 nm. It can be observed that the distant between two grooves should be at least 2.5 nm for the scratching depth of 5 nm in order to avoid interference. The simulations were also conducted for the different scratching depths and crystal orientations. Based on the results, it could be concluded that the minimum distant between two scratched grooves should be at least half of the scratching depth and irrespective crystal orientation.

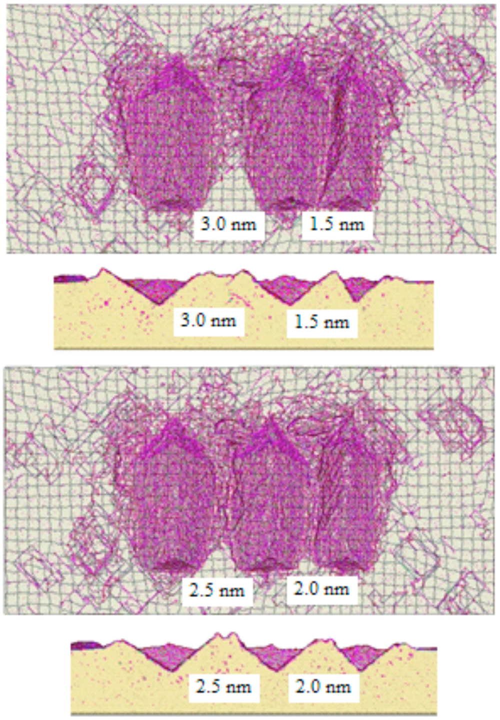

Figure 4: MD simulation snapshots of nano-scratching with various distant between two scratched grooves

Figure 5 shows the variation in normal force with the scratch length at different depths. It can be seen that the normal force, obtained from MD simulations, increases with scratch length.

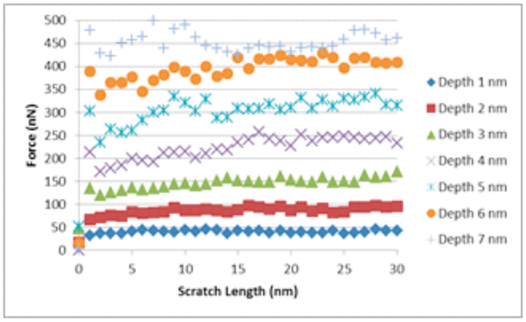

Figure 5: Variation in normal forces with scratch length at different depthes of scratch

The AFM-based nanomachining has also been applied to the fabrication of nanofluidic devices. AFM was used to create nanochannels by directly scratching on the surface of the sample. Figure 6 shows AFM images of nanochannels conducted with different applied forces, scratching length, and feed rates.

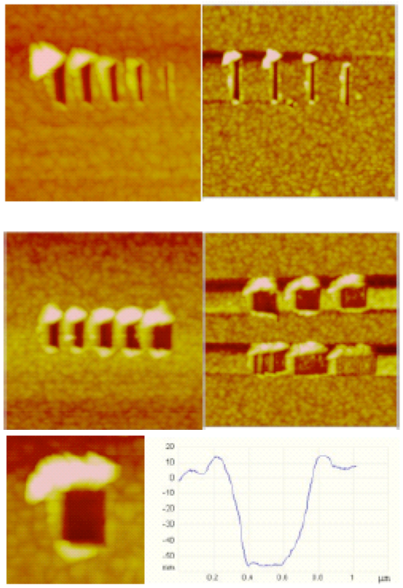

Figure 6: AFM images of nano-channels

After creating the nanochannels between the two micro-channels, the devices were sealed using PDMS (polydimethylsiloxane). Figure 7 shows the device after PDMS bonding process. Fluid flow test was conducted on the devices. SP101L syringe pump was used to pump the fluid through 0.05-inch internal diameter pipe, which is connected, to inlet reservoir of micro-channel as shown in Figure 8. When the fluid is poured inside the pipe at the rate of 50 micrometer/second, it passes through the micro-channels and nanochannels to the outlet reservoir of micro-channel. The device after fluid test is shown in Figure 9.

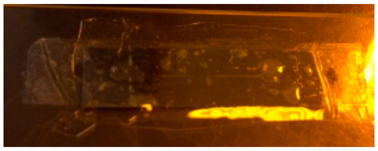

Figure 7: PDMS sealed on the device

Figure 8: Fluid flow test setup

Figure 9: Device after fluid test

4 CONCLUSION

MD simulations of AFM-based nanoscratching were conducted to investigate the effect of scratching depth and distance between any two scratched grooves. Several types of defects, including vacancies and Shockley partial dislocation loops, could be observed during the simulation. With increasing depth of scratch, the dislocations reach side boundaries sooner and re-enter from the opposite side. Some of these partial dislocations interact with other defects to form more defects on the top surface. The simulation also allows for the prediction of normal force at the interface between the indenter and substrate. The normal force increases as the scratch length increases In addition, the AFM-based nanoscratching was applied to the fabrication of nanochannels. The resulting nanochannels/ nano-fluidic devices were tested for proper operation and then used in the study of DNA analysis.

REFERENCES

[1] A. N. Shipway, E. Katz and I Willner, “Nanoparticle Arrays on Surfaces for Electronic, Optical, and sensor applications,” *ChemPhysChem* Vol. 1(1), pp. 18–52, 2000.

[2] M. Liu, N. A. Amro, C. S. Chow and G-Y Liu, “Production of Nanostructures of DNA on Surfaces,” *Nano Letters*, Vol. 2(8), pp. 863–867, 2002.

[3] P. Vettiger, M. Despont, U. Drechsler, U. Dürig, W. Häberle, M. I. Lutwyche, H. Rothuizen, R. Stutz, R. Widmer and G. K. Binnig, “The ‘millipede’ – more than one thousand tips for future AFM data storage,” *IBM Journal of Research and Development*, Vol. 44(3), pp. 323–340, 2000.

[4] C. R. Taylor, E. A. Stach, G. Salamo and A. P. Malshe, “Nanoscale dislocation Patterning by Ultralow Load Indentation,” *Applied Physics Letters*, Vol. 87(7), 073108, 2005.

[5] G. F. Zheng, F. Patolsky, Y. Cui, W. U. Wang and C. M. Lieber, “Multiplexed electrical detection of cancer markers with nanowire sensor arrays,” *Nature Biotechnology*, Vol. 23(10), pp. 1294-1301, 2005.

[6] X. Li, H. Gao, C. J. Murphy and K. K. Caswell, “Nanoindentation of silver nanowires,” *Nano Letters*, Vol. 3, pp.1495-1498, 2003.

[7] X. Li, P. Nardi, C. W. Baek, J. M. Kim and Y. K. Kim, “Direct nanomechanical machining of gold nanowires using a nanoindenter and an atomic force microscope,” *Journal of Micromechanics and Microengineering*, Vol. 15, pp. 551-556, 2005.

[8] Y. D. Yan, T. Sun, X. S. Zhao, Z. J. Hu and S. Dong, “Fabrication of microstructures on the surface of a micro/hollow target ball by AFM,” *Journal of Micromechanics and Microengineering*, Vol. 18, 035002, 2008.

[9] Y. J. Chen, J. H. Hsu and H. N. Lin, “Fabrication of metal nanowires by atomic force microscopy nanoscratching and lift-off process,” *Nanotechnology*, Vol. 16, pp. 1112-1115, 2005.

[10] Y. T. Mao, K. C. Kuo, C. E. Tseng, J. Y. Huang, Y. C. Lai, J. Y. Yen, C. K. Lee and W. L. Chuang, “Research on three dimensional machining effects using atomic force microscope,” *Review of Scientific Instruments*, Vol. 80, 065105, 2009.

[11] T. Fang, C. Weng and J. Chang, “Machining characterization of nano-lithography process using atomic force microscopy,” *Nanotechnology*, Vol. 11, pp. 181-187, 2000 [1] Timoshenko and Woinowski-Krieger, "Theory of Plates and Shells," McGraw-Hill, 415-4215, 1959.

[12] L. Jay Guo, X. Cheng, and C.F. Chou, “Fabrication of size-controllable nanofluidic channels by nanoimprinting and its application for DNA stretching,” *Nano Letter*, Vol. 4, pp. 69-73, 2004.

[13] S. J. Plimpton, “Fast parallel algorithms for short-range molecular dynamics,” *Journal of Computational Physics*, Vol. 117, pp. 1-19, 1995.

[14] S. J. Plimpton, R. Pollock and M. Stevens, “Particle-mesh Ewald and rRESPA for parallel molecular dynamics simulations,” *Proc of the Eighth SIAM Conference on Parallel Processing for Scientific Computing, Minneapolis*, MN, 1997.

[15] P. Walsh, R. K. Kalia, A. Nakano and P. Vashishta, “Amorphization and anisotropic fracture dynamics during nanoindentation of silicon nitride: A multimillion atom molecular dynamics study,” *Applied Physics Letters*, Vol.77, pp.4332-4334, 2000.

[16] Tersoff, J., “New empirical approach for the structure and energy of covalent systems,” *Physical Review B*, Vol. 37, pp. 6691-7000, 1988.

[17] J. Li, “AtomEye: an efficient atomistic configuration viewer,” *Modeling and Simulation in Materials Science and Engineering*, Vol. 11, pp. 173-177, 2003.